Selective control of polarized emission from patterned GaN/AlN quantum dot ensembles on Si(111)

O. Moshe,[1] D. H. Rich,[1,a)] B. Damilano,[2] and J. Massies[2]
[1]*Department of Physics and The Ilse Katz Institute for Nanoscale Science and Technology, Ben-Gurion University of the Negev, P.O. Box 653, Beer-Sheva 84105, Israel*
[2]*Centre de Recherche sur l'Hétéro-Epitaxie et ses Applications, Centre National de la Recherche Scientifique, Rue B. Gregory, Sophia Antipolis, 06560 Valbonne, France*

(Received 6 January 2011; accepted 20 January 2011; published online 9 February 2011)

GaN/AlN quantum dots (QDs) were grown by the Stranski–Krastanov method on Si(111). The thermal expansion coefficient mismatch between the Si substrate and GaN/AlN film leads to an additional biaxial tensile stress of 20–30 kbar in the III-nitride film, which we have selectively modified by etching a cross-hatched pattern into the as-grown sample. The results show that a suitable choice of stripe orientation and width from ~2 to 10 μm can create regions of in-plane uniaxial stress that enable a selective and local control of the polarized luminescence from ensembles of QDs which were probed with cathodoluminescence. © *2011 American Institute of Physics*. [doi:10.1063/1.3554371]

In the past decade, much emphasis has been placed on the growth, characterization, and theory of GaN/AlN-based wurtzite self-assembled quantum dots (QDs) as a result of potential solid-state light emitting applications in the visible wavelength range.[1–3] An important characteristic of group III-nitride compounds is the existence of a large polarization field, originating from both piezoelectric and spontaneous polarizations.[4,5] Recently, we demonstrated that randomly generated microcracks along ⟨11−20⟩ in GaN/AlN QD layers grown on Si(111) can serve as excellent stressors which create an in-plane uniaxial stress of 20–30 kbar in limited regions of the III-nitride film.[6–9] Moreover, in close proximity (i.e., within a few micrometers) to the microcracks the excitonic luminescence from the GaN QDs is partially linearly polarized, as a result of the uniaxial stress.[7–10] The effect of an in-plane uniaxial stress on GaN/AlN QDs has also been examined theoretically.[11]

The development of III-nitride-based light emitting diodes (LEDs) with polarized light emission is a topic of current interest with immediate applications in backlit nematic-phase liquid-crystal displays (LCDs). Exploiting polarized III-nitride-based LEDs in LCD systems could yield a substantial increase in power efficiency for the display system by eliminating the need for polarization filters. Polarized monochromatic light can be generated by InGaN-based LEDs grown on nonpolar orientations such as the (1−100) *m*-plane GaN face.[12,13] Optical intensity modulation of nonpolar InGaN LEDs by an LCD system has been demonstrated.[14] Consequently, an added motivation for the implementation of III-nitride QD polarized LEDs fabricated on standard Si(111) substrates is for potential applications in large area LCD systems, which could benefit economically from the integration of III-nitride QD films with Si microelectronics.[15] In this letter, we demonstrate that post-growth patterning of GaN QD ensembles grown on Si(111) can be used to selectively modify the thermal stress in the III-nitride film and induce polarized luminescence from QD ensembles.

The GaN/AlN QD sample was grown by molecular beam epitaxy using the Stranski–Krastanov growth mode transition. The sample was grown on Si(111) and consists of AlN (30 nm)/GaN (400 nm)/AlN (700 nm) buffer layers followed by 85 layers of GaN QDs, labeled as sample S85. The growth involved 6.7 nm thick AlN barrier layers with 1.6 nm thick GaN QD layers, resulting in an average dot height of ~3.7 nm and an average dot density per QD plane of $\sim 5 \times 10^{11}$ cm^{-2}.[6–9] SiO_2 and photoresist mask patterns were formed on the sample, through which the GaN/AlN QD layers were selectively etched until the underlying Si substrate was exposed. Inductively coupled Cl_2/Ar plasma reactive ion etching was used to etch into the as-grown sample a cross-hatched pattern consisting of square trenches of area equal to 20×20 μm^2 having stripes of varying widths with edges along the orthogonal in-plane [11−20] and [1−100] directions. The spacing between the edges of the square trenches was intentionally varied to create vertical and horizontal stripes having widths ranging from ~2 to 10 μm. The widths of adjacent parallel stripes decrease by ~1 μm in both left-to-right and top-to-bottom sequences of the cross-hatched pattern, as observed in Fig. 1.

Our cathodoluminescence (CL) detection system is mounted on a JEOL 5910 scanning electron microscope (SEM).[6–9] Two polarization directions for the polarizer will be denoted with the subscripts ⊥ and ∥ to indicate detection orientations with **E** perpendicular and parallel to a stripe along [11−20]. The polarization anisotropy ratio R_p is defined by the ratio of the integrated CL intensities I under the two orthogonal polarizer orientations and is given by $R_p = I_\perp / I_\parallel$. The CL spectra and images were acquired with an *e*-beam energy (E_b) of 15 keV and a beam current (I_b) of 300 pA. The spectral resolution of the monochromator was 2 nm (~15 meV) at λ=400 nm (3.100 eV). Time-resolved CL experiments were performed with the method of delayed coincidence in an inverted single photon counting mode.[9]

The patterned region that was probed with CL is shown in the SEM and polarization anisotropy ratio images of Figs. 1(a)–1(d). A magnified portion of the dashed rectangle in Fig. 1(a) is shown in Fig. 1(b). The horizontal and vertical

a)Electronic mail: danrich@bgu.ac.il.

Author complimentary copy. Redistribution subject to AIP license or copyright, see http://apl.aip.org/apl/copyright.jsp

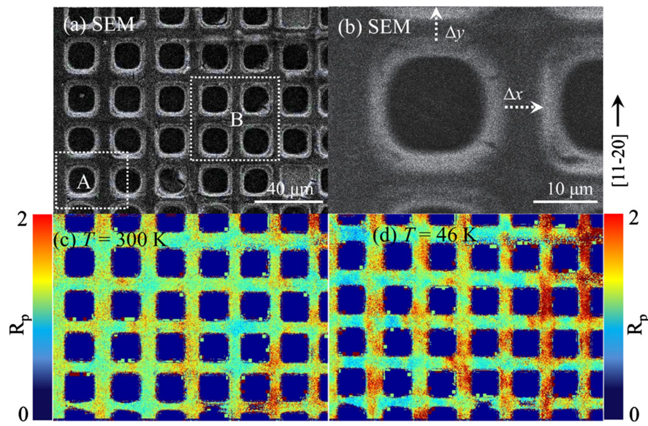

FIG. 1. (Color online) SEM micrographs in (a) and (b) showing the cross-hatched pattern with square trenches etched into the GaN/AlN QD sample. Region A in (a), indicated with the dashed rectangle, is shown with higher magnification in (b). Region B in (a), indicated with a dashed square, corresponds to a rectangular region analyzed with AEI and CLWI in Fig. 3. CL polarization anisotropy ratio images, $R_p = I_\perp(x,y)/I_\parallel(x,y)$, are shown in (c) and (d) for sample temperatures of 300 and 46 K, respectively.

dashed lines in Fig. 1(b) indicate paths on which the focused e-beam was positioned for localized CL spectroscopy measurements. Local CL spectra at $T=46$ K, acquired under $\mathbf{E}\perp$ [11−20] and $\mathbf{E}\parallel$ [11−20] detection orientations, are shown in Fig. 2 for various e-beam positions along the center of vertical and horizontal stripes that connect adjacent square trenches. The distances Δx and Δy indicate distances from the beginning of the dashed horizontal and vertical lines in Fig. 1(b) on which the e-beam was focused during the acquisition of the local CL spectra of Fig. 2. The polarization anisotropy is evident in Fig. 2(a) by the ratios R_p, which vary from 1.53 to 1.75 for each set of CL spectra acquired along the vertical stripe (i.e., increments along the Δx direction). A similar result is observed for CL spectra acquired for excitation on the orthogonal stripe with increments along the Δy direction, as observed in Fig. 2(b).

The spatial distribution of the polarization anisotropy ratio R_p was further examined by acquiring monochromatic CL images at $h\nu=3.00$ eV under $\mathbf{E}\perp$ [11−20] and $\mathbf{E}\parallel$ [11−20] detection orientations. The images of Figs. 1(c) and 1(d), with the sample maintained at temperatures of 300 and 46 K, respectively, show ratios $R_p = I_\perp(x,y)/I_\parallel(x,y)$ for each 640×480 pixel image. The false color bar is used to map R_p and shows variations in R_p between adjacent vertical and horizontal stripes exhibiting varying widths for the two sample temperatures. A clear reversal in the polarization anisotropy is seen near the centers of horizontal and vertical stripes, consistent with the polarized CL spectra shown in Fig. 2. Moreover, the largest values of R_p ($R_p\approx2$) are observed for the narrowest stripes with widths approaching $\sim$4 μm toward the right in Fig. 1(d), owing to a more complete stress relief (i.e., $\sigma_{xx}\approx0$) along the stripe's orthogonal direction near its center. An increase in R_p is observed near the centers of the stripes as the temperature is reduced from 300 to 46 K. An increase in uniaxial tensile stress at low temperatures is expected to occur due to the further contraction of the GaN/AlN film relative to the Si substrate and leads to an increase in R_p near the centers of the stripes. A similar temperature dependence of R_p was observed in close proximity to microcracks in sample S85, again as a result of an increase in uniaxial stress during sample cooling.[7,8,10] In most cases, the intersections of horizontal and vertical stripes yield an $R_p\approx1$, which is consistent with the presence of biaxial stress (i.e., $\sigma_{xx}\approx\sigma_{yy}$). Some exceptions can be found, particularly at $T=46$ K, owing to a possible anisotropic contraction of the QD layers in the cross-hatched pattern during cooling.

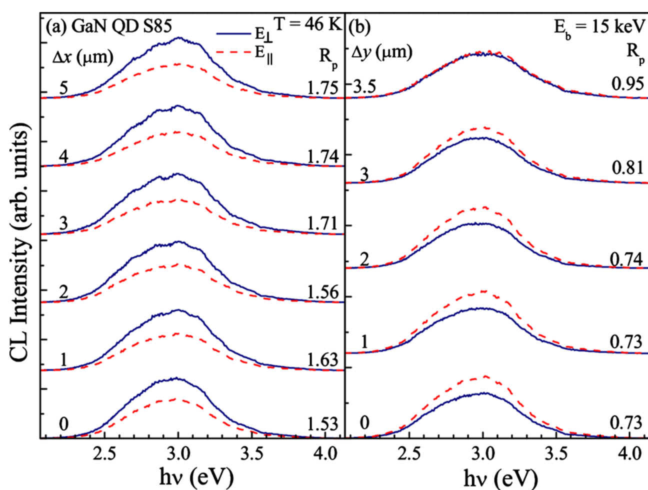

FIG. 2. (Color online) Stack plots of CL spectra acquired with polarization detection orientations of $\mathbf{E}\perp$ [11−20] and $\mathbf{E}\parallel$ [11−20] for the e-beam focused at various positions, Δx and Δy, along the vertical and horizontal stripes shown in Fig. 1(b). The polarization anisotropy ratio, $R_p = I_\perp/I_\parallel$, is shown for each set of CL spectra acquired at the indicated Δx and Δy in (a) and (b), respectively.

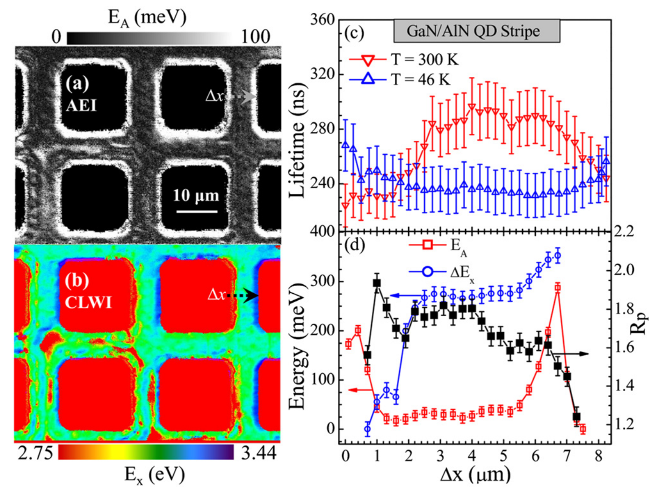

FIG. 3. (Color online) AEI and CLWI in (a) and (b), respectively. The images were acquired in the region denoted by the dashed square labeled B in the SEM image of Fig. 1(a). The mapping of E_A and E_x is shown with the gray and false color bars, respectively. A linescan analysis along the region marked with an arrow in (b) is shown in (c) for the QD e-h lifetime and in (d) for E_A, ΔE_x, and R_P. The CLWI and R_P linescan measurements were performed at $T=46$ K.

Other salient features of the data are observed in the activation energy imaging (AEI) and CL wavelength imaging (CLWI) modes shown in Figs. 3(a) and 3(b). In AEI, the activation energy E_A for the thermal quenching of the QD luminescence in the $220\leq T\leq300$ K is determined and mapped for each (x,y) pixel.[6,8] Previously, we showed that E_A is sensitive to the stress profile in the film due to the presence of defect states in the AlN barrier band gap, whose energy positions relative to the QD confined electron and hole states are sensitive to the total strain in the III-nitride

Author complimentary copy. Redistribution subject to AIP license or copyright, see http://apl.aip.org/apl/copyright.jsp

film.[8] The CLWI shown in Fig. 3(b) likewise maps the energy position of the excitonic peak, E_x, of the QD luminescence ($T=46$ K), which is again expected to vary according to changes in the QD strain tensor. While the AEI mode shows an increase in E_A near the edges of the square trenches, CLWI reveals an asymmetric behavior in which a relative redshift and blueshift in E_x are observed for the left and right edges, respectively, of the vertical stripes in Fig. 3(b).

Time-resolved CL was performed on a vertical stripe as a function of *e*-beam position along the dashed line in Fig. 3(b), enabling a linescan measurement of the QD *e-h* lifetime,[6,9,10] as shown in Fig. 3(c). An interesting behavior is observed near the center of the stripes ($\Delta x \approx 4$ μm) in which the lifetimes at $T=300$ K are ~20% larger than those in the same position for $T=46$ K. The decrease in the decay time at low temperature is at first glance somewhat perplexing since the reduction of the *nonradiative* components at lower temperatures ought to increase the overall decay time. However, again we consider the ever increasing thermal tensile stress of the III-nitride film in the middle of the stripe as the temperature is lowered from 300 to 46 K. The increasing thermal tensile stress of the AlN barriers is expected to reduce the compressive stress of the GaN QDs, thereby resulting again in a reduced electric field responsible for the spatial separation of electrons and holes. Thus, we hypothesize that a field reduction at low temperatures is primarily responsible for an increased oscillator strength and a reduced carrier lifetime, as observed in Fig. 3(c).

A more complete understanding of the correlations in the various CL imaging modes is obtained by a linescan analysis, as shown in Fig. 3(d) for the AEI, CLWI, and R_p versus Δx along the positions of the dashed horizontal line shown in Fig. 3(b). In this plot, we show ΔE_x, as obtained from CLWI, so that it can be compared directly with E_A using the same energy axis. The relative redshift and blueshift observed in this linescan analysis and in the CLWI of Fig. 3(b) are attributed to an asymmetric strain relaxation near the boundaries of the square trenches. Since the resulting excitonic transition energy is a competition between strain-induced changes in the band edges and the field-induced quantum confined Stark effect, a small change in strain between opposite edges of a stripe can therefore cause either a redshift or a blueshift in E_x.[6] On the other hand, E_A is expected to behave in a monotonic fashion as a function of strain since it is primarily sensitive to changes in the AlN barrier band edges relative to the confined GaN QD ground state levels and should exhibit a weaker dependence on field.[6,8]

In conclusion, we have selectively modified the thermal-induced stress in GaN/AlN QD layers by etching a cross-hatched pattern into the as-grown sample using inductively coupled Cl_2/Ar plasma reactive ion etching. The results show that a suitable choice of stripe width from ~2 to 10 μm and orientation can create regions of in-plane uniaxial stress that enable a selective and local control of the polarized luminescence from ensembles of QDs. These results demonstrate the possibility of utilizing growth of III-nitride QDs on thermally mismatched Si as a method in strain engineering to create polarized solid-state light sources that could be incorporated into LCD technologies.

[1] S. Tanaka, H. Hirayama, Y. Aoyagi, Y. Narukawa, Y. Kawakami, and S. Fujita, Appl. Phys. Lett. **71**, 1299 (1997).
[2] B. Damilano, N. Grandjean, F. Semond, J. Massies, and M. Leroux, Appl. Phys. Lett. **75**, 962 (1999).
[3] B. Damilano, N. Grandjean, J. Massies, and F. Semond, Appl. Surf. Sci. **164**, 241 (2000).
[4] A. D. Andreev and E. P. O'Reilly, Phys. Rev. B **62**, 15851 (2000).
[5] S. Kalliakos, T. Bretagnon, P. Lefebvre, T. Taliercio, B. Gil, N. Grandjean, B. Damilano, A. Dussaigne, and J. Massies, J. Appl. Phys. **96**, 180 (2004).
[6] G. Sarusi, O. Moshe, S. Khatsevich, D. H. Rich, and B. Damilano, Phys. Rev. B **75**, 075306 (2007).
[7] O. Moshe, D. H. Rich, B. Damilano, and J. Massies, Phys. Rev. B **77**, 155322 (2008).
[8] O. Moshe, D. H. Rich, B. Damilano, and J. Massies, J. Vac. Sci. Technol. B **28**, C5E25 (2010).
[9] O. Moshe, D. H. Rich, S. Birner, M. Povolotskyi, B. Damilano, and J. Massies, J. Appl. Phys. **108**, 083510 (2010).
[10] O. Moshe, D. H. Rich, B. Damilano, and J. Massies, Phys. Status Solidi C **6**, 1432 (2009).
[11] M. Winkelnkemper, R. Seguin, S. Rodt, A. Hoffmann, and D. Bimberg, J. Phys.: Condens. Matter **20**, 454211 (2008).
[12] N. F. Gardner, J. C. Kim, J. J. Wierer, Y. C. Shen, and M. R. Krames, Appl. Phys. Lett. **86**, 111101 (2005).
[13] H. Masui, H. Yamada, K. Iso, S. Nakamura, and S. P. DenBaars, J. Phys. D: Appl. Phys. **41**, 225104 (2008).
[14] H. Masui, H. Yamada, K. Iso, J. S. Speck, S. Nakamura, and S. P. DenBaars, J. Soc. Inf. Disp. **16**, 571 (2008).
[15] P. N. Chyurlia, F. Semond, T. Lester, J. A. Bardwell, S. Rolfe, H. Tang, and N. G. Tarr, Electron. Lett. **46**, 240 (2010).

Author complimentary copy. Redistribution subject to AIP license or copyright, see http://apl.aip.org/apl/copyright.jsp